Critical current in type-II superconductors near the order-disorder transition

I. M. Babich,[1,2] E. H. Brandt,[1] G. P. Mikitik,[1,2] and E. Zeldov[3]
[1]*Max-Planck-Institut für Metallforschung, D-70506 Stuttgart, Germany*
[2]*B. Verkin Institute for Low Temperature Physics & Engineering, Ukrainian Academy of Sciences, Kharkov 61103, Ukraine*
[3]*Department of Condensed Matter Physics, Weizmann Institute of Science, Rehovot 76100, Israel*
(Received 16 November 2009; revised manuscript received 21 January 2010; published 22 February 2010)

We investigate theoretically the critical states in a long thin superconducting strip with a critical transport current and in a perpendicular magnetic field, which is close to the field of the order-disorder transition in the vortex lattice. In this investigation, the metastable disordered states and the self-magnetic-field of the current are taken into account. Using the obtained results, the dependence of the dc critical current in the strip on the applied magnetic field is found near the order-disorder transition. This dependence can be used to describe the peak effect in low-T_c superconductors and the second magnetization peak in high-T_c superconductors, which occur near this transition.

DOI: 10.1103/PhysRevB.81.054517 PACS number(s): 74.25.Uv, 74.25.Sv

I. INTRODUCTION

The peak effect, i.e., a maximum in the dependence of the critical current density on temperature T or magnetic field H, frequently occurs in low-T_c type-II superconductors not far below the upper critical field $H_{c2}(T)$.[1–7] A similar "fishtail effect" or second magnetization peak, is observed in many high-T_c superconductors but in another region of the T-H plane.[8–13] Both these effects are frequently associated with a proliferation of dislocations in the flux-line lattice.[1,2,4–6,14–22] This proliferation occurs at the order-disorder transition,[23–25] which is induced by quenched disorder in the vortex system at a certain value $B_{\rm dis}(T)$ of the local magnetic induction, see also Ref. 26 and the papers cited therein. At this transition, with increasing H or T the flux-line lattice transforms from the quasiordered Bragg glass[27] into the disordered amorphous vortex phase. Under this transformation the flux-line pinning increases, leading to an abrupt increase of the critical current density j_c at the induction $B_{\rm dis}$. With this increase and the natural assumption that j_c in the disordered phase decreases with increasing magnetic induction and temperature, one arrives at a qualitative explanation of the peak and fishtail effects.

Near the order-disorder transition various unusual phenomena were observed in type-II superconductors.[28–35] In the paper of Paltiel *et al.*,[4] the following mechanism was proposed that qualitatively explains all these phenomena: in the presence of a perpendicular external magnetic field and of a transport current, vortices penetrate from one edge of the sample and leave it at the opposite edge. The penetrating vortices are injected at the weakest points of the surface barrier, thereby destroying the local order and forming a metastable disordered vortex phase near the edge even at $B < B_{\rm dis}$. This disordered phase drifts into the sample with the flow of the entire vortex lattice under the action of the current flowing in the bulk. On the other hand, this drift acts as an annealing mechanism. Thus, the state of the vortex lattice in the superconductor is determined by the competition between the injection of the disordered vortex phase at the edges of a platelet-shaped sample, and the dynamic annealing of this metastable disorder by the vortex motion. As a result, a nonuniform distribution of the disordered and ordered phases is established in the sample. This distribution is characterized by the annealing length L_a, which *decreases* with increasing vortex-lattice velocity v.[30,36] Note that the role of thermal fluctuations in the annealing is completely disregarded within this approach. This neglect of the thermal fluctuations is well justified in low-T_c superconductors such as $NbSe_2$.

The described contamination-annealing model does not change essentially if the annealing of the metastable disordered phase is due to the thermal fluctuation of the vortices. This situation is realized, e.g., in $Bi_2Sr_2CaCu_2O_{8+\delta}$ (BSCCO) superconductors. The order-disorder transition in these crystals manifests itself as a break in the slope of the magnetic field profiles measured on the upper surface of the sample.[23,37,38] But the magnetic induction at which the break occurs depends on experimental conditions.[39–42] This fact points to the existence of the so-called transient (metastable) disordered vortex states in the sample.[39,40] As it was shown in Ref. 41, the experimental data measured at different sweep rates of the external magnetic field (at different velocities v of the vortex lattice) can be understood within the contamination-annealing model if one uses the following annealing time τ_a for the metastable disordered phase at temperature T and the magnetic induction $B < B_{\rm dis}$,

$$\tau_a \approx \tau_0(T)\left(1 - \frac{B}{B_{\rm dis}}\right)^{-\gamma}, \qquad (1)$$

where $\gamma = 2.6$ and $\tau_0 = 8 \times 10^{-9} \exp(326/T)$ s. For $B > B_{\rm dis}$ the disordered phase is stable and τ_a is infinite. In the case of expression (1) the annealing length $L_a = v\tau_a$ *increases* with increasing v, which proves that the dynamic annealing does not play an essential role in the experiments with BSCCO crystals.

In analyzing critical states of thin superconducting platelets in a perpendicular magnetic field an essential point is to take properly into account the self fields of the critical currents. In $NbSe_2$ crystals, the critical current densities are small, and so these fields are negligible in the peak-effect region. Neglecting these fields, the critical current of a superconducting strip in the peak-effect region was theoretically analyzed in Ref. 36 within the contamination-annealing model described above. But the fields of the currents need not be small for all superconductors. For example, these fields may be essential near the order-disorder transition in BSCCO crystals. Near this transition the critical states of a strip in an increasing or a decreasing external magnetic field H_a were analyzed numerically[43] and analytically,[44] taking into account the fields of the currents. But the analysis was carried out only in the limit when τ_a, $L_a=0$ for any $B<B_{\rm dis}$ and τ_a, L_a are infinite for $B>B_{\rm dis}$, which means that at every point of the strip a local equilibrium is established, i.e., the critical value of the sheet current is determined by the local magnetic induction,

$$J_c(B_z)=J_{c1} \ \text{ for } \ B_z<B_{\rm dis},$$

$$J_c(B_z)=J_{c2} \ \text{ for } \ B_z>B_{\rm dis}, \tag{2}$$

where J_{c1}, J_{c2} (with $J_{c2}>J_{c1}$) are the sheet currents in the ordered and disordered phases, respectively. In other words, in this local-equilibrium model the metastable disordered states are disregarded. But an essential feature of this model is an extended spatial region where $B_z=B_{\rm dis}$, and in this region a distribution of the ordered and disordered phases still occurs although both phases are stable there. However, even in this local-equilibrium model the critical current of the strip was not calculated since critical states with a transport current were not considered.

In this paper, we theoretically study the critical current of the superconducting strip near the order-disorder transition in the general case, taking into account both the metastable disordered states and the self-magnetic-fields of the current. But we begin our investigation with solving the appropriate critical state problem within the local-equilibrium model (τ_a, $L_a\to 0$ at $B_z<B_{\rm dis}$) and calculating the critical current I_c in this special case. Then, we consider the contamination-annealing model ($\tau_a>0, L_a>0$), taking into account the self fields of the currents, and show how the analytical results obtained in the local equilibrium approximation are related to the general results at finite τ_a and L_a. In our analysis we consider the situation when an increasing external magnetic field H_a is first switched on, and then the critical transport current is applied to the sample. For definiteness, we also assume that the thermal fluctuations play the main role in the annealing process and use the dependence [Eq. (1)] with $\gamma=2.6$ for $\tau_a(B_z)$. Beside this, throughout the paper, we imply the relationship $B=\mu_0 H$ between the magnetic induction B and the magnetic field H, that is, we neglect the equilibrium magnetization. For simplicity, J_{c1} and J_{c2} are considered as constants independent of B_z until the final section of the paper.

II. LOCAL EQUILIBRIUM MODEL

Consider a superconductor that has the shape of infinitely long strip of width $2w$ and of thickness $d\ll w$, with the x axis being along the width of the strip ($-w\le x\le w$), and with the z axis being normal to the strip plane (inside the strip one has $-d/2\le z\le d/2$). The external magnetic field H_a is applied along the z axis. Let a local equilibrium occur in the sample. In other words, the local critical sheet current is determined by the local value of B_z according to Eq. (2). Let us calculate the critical current of the strip, $I_c(H_a)$, taking into account the self fields of the critical currents. According to the Biot–Savart law, the magnetic field in the strip is expressed in terms of the sheet current $J(x)$ (the current density integrated over the thickness d) as follows:

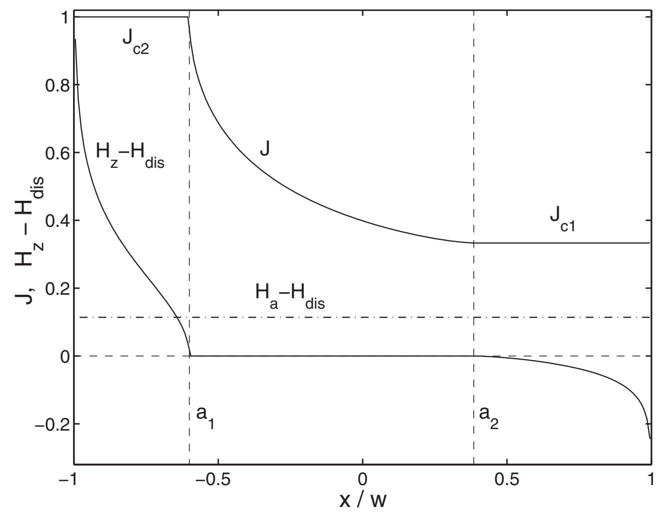

FIG. 1. Profiles of the critical sheet current $J(x)$ and of the magnetic field $H_z(x)$ in the strip within the local equilibrium model. The sheet current and the magnetic field are measured in units of J_{c2}. Here $J_{c1}/J_{c2}=1/3$ and $(H_a-H_{\rm dis})/J_{c2}=0.114$. This gives $a_1=-0.6w$ and $a_2=0.3846w$.

$$H_z(x)=H_a+\frac{1}{2\pi}\int_{-w}^{w}\frac{J(x')dx'}{x'-x}. \tag{3}$$

This equation should be supplemented by the critical state conditions,

$$J(x)=J_{c2} \ \text{ for } \ -w\le x\le a_1, \tag{4}$$

$$H_z(x)=H_{\rm dis} \ \text{ for } \ a_1\le x\le a_2, \tag{5}$$

$$J(x)=J_{c1} \ \text{ for } \ a_2\le x\le w. \tag{6}$$

Here $x=a_1$ defines the boundary of the region where $J(x)=J_{c2}$ and $H_z(x)>H_{\rm dis}$, i.e., where the disordered vortex phase exists, while $x=a_2$ describes the boundary of the ordered phase region where $J(x)=J_{c1}$ and $H(x)<H_{\rm dis}$, Fig. 1. At these boundaries the field H reaches $H_{\rm dis}$. At $a_1\le x\le a_2$ one has $H(x)=H_{\rm dis}$, while the sheet current lies in the interval $J_{c1}\le J\le J_{c2}$. In this region, a mix of the ordered and disordered phases exists. Note that the regions of the completely ordered and disordered phases do not contact each other immediately, i.e., $a_1\ne a_2$. Otherwise, the condition (2) for local equilibrium would not agree with Eqs. (4)–(6).[44,45] Eqs. (3)–(6) lead to a linear singular integral equation with Cauchy-type kernel for the current $J(x)$ at $a_1\le x\le a_2$. Similarly to Ref. 44, we find the solution of this equation using the theory of such singular integral equations.[46] Here, we present the final results.

The sheet current at $a_1 \le x \le a_2$ has the form,

$$J(x) = \frac{2J_{c1}}{\pi}\arctan\frac{\sqrt{w-a_2}\sqrt{x-a_1}}{\sqrt{w-a_1}\sqrt{a_2-x}} + \frac{2J_{c2}}{\pi}\arctan\frac{\sqrt{w+a_1}\sqrt{a_2-x}}{\sqrt{w+a_2}\sqrt{x-a_1}}, \qquad (7)$$

[while $J(x)=J_{c1}$ at $w \ge x \ge a_2$, and $J(x)=J_{c2}$ at $a_1 \ge x \ge -w$]. The magnetic field outside the interval $a_1 \le x \le a_2$ is given by

$$H_z(x) = H_a + \frac{J_{c1}}{\pi}\ln\frac{\sqrt{|w-x|}(\sqrt{w-a_1}+\sqrt{w-a_2})}{\sqrt{w-a_1}\sqrt{|a_2-x|}+\sqrt{w-a_2}\sqrt{|a_1-x|}} + \frac{J_{c2}}{\pi}\ln\frac{\sqrt{w+a_2}\sqrt{|a_1-x|}+\sqrt{w+a_1}\sqrt{|a_2-x|}}{\sqrt{|w+x|}(\sqrt{w+a_2}+\sqrt{w+a_1})}, \qquad (8)$$

[while $H_z(x)=H_{\rm dis}$ at $a_1 \le x \le a_2$]. The region boundaries a_1 and a_2 are found from the equations,

$$\frac{a_2}{w} = \frac{w(J_{c2}^2-J_{c1}^2)+a_1(J_{c2}^2+J_{c1}^2)}{w(J_{c2}^2+J_{c1}^2)+a_1(J_{c2}^2-J_{c1}^2)}, \qquad (9)$$

$$H_{\rm dis} = H_a + \frac{J_{c1}}{\pi}\ln\frac{\sqrt{w-a_1}+\sqrt{w-a_2}}{\sqrt{a_2-a_1}} + \frac{J_{c2}}{\pi}\ln\frac{\sqrt{a_2-a_1}}{\sqrt{w+a_1}+\sqrt{w+a_2}}. \qquad (10)$$

Formulas (7)–(10) completely describe the critical state in a strip carrying the critical current $I_c=\int_{-w}^{w}J(x)dx$, Fig. 1. Using these formulas, we find two equivalent expressions for this critical current,

$$I_c(H_a) = J_{c1}\sqrt{w-a_1}\sqrt{w-a_2}+J_{c2}\sqrt{w+a_1}\sqrt{w+a_2} = \sqrt{2J_{c1}^2 w(w-a_1)+2J_{c2}^2 w(w+a_1)}, \qquad (11)$$

where $a_1(H_a)$ and $a_2(H_a)$ are found from Eqs. (9) and (10). Figure 2 shows the magnetic-field dependence of the dc critical current I_c in the local equilibrium model. This dependence reveals a plateau rather than a peak in I_c because we have not yet included the H dependences of J_{c1} and J_{c2} in our analysis.

To get a deeper insight into the obtained results, consider the limiting case $J_{c2} \gg J_{c1}$. In this case formulas (7)–(11) simplify, and we find for I_c the following approximate expressions:

$$I_c(H_a) \approx 2wJ_{c2}\tanh\left[\frac{\pi(H_a-H_{\rm dis})}{J_{c2}}\right], \qquad (12)$$

$$I_c(H_a) \approx 2wJ_{c1}\left\{1+2\exp\left[\frac{2\pi(H_a-H_{\rm dis})}{J_{c1}}-2\right]\right\}, \qquad (13)$$

at $H_a-H_{\rm dis} \gg J_{c1}/\pi$ and $H_a-H_{\rm dis} < -J_{c1}/\pi$, respectively. In this case, the H_a-dependence of the critical current mainly develops on the characteristic scale J_{c2}/π. At the order-disorder transition the critical current is considerably less than its maximum value $2wJ_{c2}$, and one has $I_c(H_a=H_{\rm dis}) \approx 2.45wJ_{c1}$. According to Eqs. (12) and (13), the curve

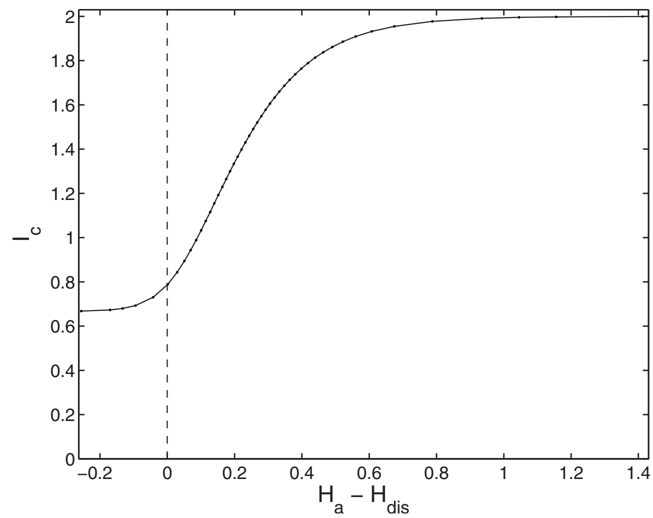

FIG. 2. The magnetic field dependence of the critical current I_c of the strip within the local equilibrium model at $J_{c1}/J_{c2}=1/3$. The critical current I_c is measured in units of wJ_{c2} and the external magnetic field H_a in units of J_{c2}.

$I_c(H_a)$ is concave at $H_a-H_{\rm dis}<0$ and convex at $H_a-H_{\rm dis}>0$. Thus, in this limiting case the point of the order-disorder transition, $H_{\rm dis}$, is close to the inflection point of $I_c(H_a)$. Interestingly, in the magnetic hysteresis loop, $M_z(H_a)$, calculated for a strip without transport current the transition point $H_{\rm dis}$ practically coincides with the point at which $d^2M_z(H_a)/dH_a^2$ is maximum.[44]

III. CONTAMINATION-ANNEALING MODEL

We calculate now the critical current of the strip within the contamination-annealing model, i.e., taking into account the metastable disordered states at $B<B_{\rm dis}$. These states decay with distance from the strip boundary at which vortices are injected into the sample. As in Ref. 36, we shall describe the annealing stage of the disordered phase by its local critical sheet current $J_c(x)$, which has a nonequilibrium excess value $\tilde{J}_c(x)=J_c(x)-J_{c1}$ relative to the fully annealed ordered phase. Let a dc electric field E be applied to the strip, and this E generates a dc transport current flowing in the sample. Using a simple model in which E is proportional to $J-J_c$ at $J \ge J_c$, the sheet current at the point x can be written in the form

$$J(x) = J_c(x) + \frac{E\cdot d}{\rho_{\rm ff}}, \qquad (14)$$

where $\rho_{\rm ff}$ is the flux-flow resistivity. For simplicity, we assume here that $\rho_{\rm ff}$ is the same for the ordered and the disordered phases. Since $1/\tau_a$ is, by definition, $-(1/\tilde{J}_c)(d\tilde{J}_c/dt)$ where d/dt is the time derivative in the coordinate system moving together with the vortices, the critical sheet current $J_c(x)$ is determined by the following differential equation describing the annealing process,

$$v\frac{\partial \tilde{J}_c(x)}{\partial x} = -\frac{\tilde{J}_c(x)}{\tau_a(B_z)}, \tag{15}$$

where $v(x)=E/B_z(x)$ is the velocity of the vortex flow. In the left hand side of Eq. (15) we have omitted the time derivative $\partial\tilde{J}_c/\partial t$ since we consider a steady flow of vortices in the strip. According to this equation, the critical sheet current tends to relax to the value J_{c1} in the region where $B_z < B_{\rm dis}$. On the other hand, if $B_z(x) > B_{\rm dis}$, the disordered phase is stable, τ_a is infinite, and $J_c(x)=J_{c2}$ for such x. The critical sheet current is equal to J_{c2} also at the injection point. So, if the vortices penetrate into the sample at $x=-w$ (i.e., if the dc transport current flows in the positive direction of the y axis), the boundary condition to Eq. (15) is

$$\tilde{J}(-w,0) = J_{c2} - J_{c1} \equiv \Delta J_c. \tag{16}$$

The solution of Eqs. (15) and (16) has the form,

$$J_c(x) = \Delta J_c \exp\left\{-\int_{-w}^{x}\frac{dx'}{L_a[B_z(x')]}\right\} + J_{c1}, \tag{17}$$

where L_a is the B_z-dependent annealing length,

$$L_a(B_z) = v\tau_a(B_z) = \frac{E\tau_a(B_z)}{B_z}. \tag{18}$$

In fact, formula (17) together with the Biot-Savart law [Eq. (3)] are a set of integral equations for $J_c(x)$ and $B_z(x) = \mu_0 H_z(x)$ which have to be solved self-consistently. On obtaining the solution of these equations and after integrating Eq. (14) over the width $2w$, one arrives at a nonlinear dc voltage-current characteristic of the superconductor, $I(E)$, within the contamination-annealing model and taking into account the self-magnetic-fields of the currents. The dc critical current I_c is obtained from this characteristic when E (and hence v) tends to zero, or in practice, to a small threshold value E_c determined by the experimental resolution.

IV. ANALYSIS

We now discuss the dc critical current I_c in detail. Let us define the magnetic field H_* by the relationship,

$$\frac{w}{L_a(H_*)} = \frac{wB_{\rm dis}}{E_c\tau_0}\left(\frac{H_*}{H_{\rm dis}}\right)\left(1-\frac{H_*}{H_{\rm dis}}\right)^{\gamma} = 1, \tag{19}$$

where $\gamma=2.6$, and we have used expressions (18) and (1) for L_a and τ_a. Equation (19) determines the ratio $H_*/H_{\rm dis}$ in terms of the only dimensionless combination of the parameters, $wB_{\rm dis}/(E_c\tau_0)$, which depends on the threshold E_c, the half-width of the strip w, and the temperature T. For example, if $w=0.6$ mm, $B_{\rm dis}=460$ G, and $E_c=6\times10^{-4}$ V/m, one obtains $wB_{\rm dis}/(E_c\tau_0)\approx 33$ and $H_*/H_{\rm dis}\approx 0.7$ at $\tau_0=1.4\times10^{-3}$ s (such τ_0 occurs[41] in BSCCO at temperature 27K). To understand the meaning of H_*, consider the behavior of L_a upon increasing the magnetic field for given values of E_c and T. For $H \ll H_{\rm dis}$ the annealing length is very small. With increasing field, L_a increases until at H_* it becomes equal to the half-width of the sample, w, and eventually it diverges at $H_a \to H_{\rm dis}$. Thus, the difference $H_{\rm dis}-H_*$ specifies the characteristic scale of the H_z dependence of L_a, and the critical current $I_c(H_a)$ increases just in the vicinity of the field H_*. We also emphasize that the parameters w, E_c, and τ_0 enter into Eq. (17) only via the combination $wB_{\rm dis}/E_c\tau_0$, and hence, the dependences of the critical sheet current on all these parameters is described by its dependence on $H_*/H_{\rm dis}$.

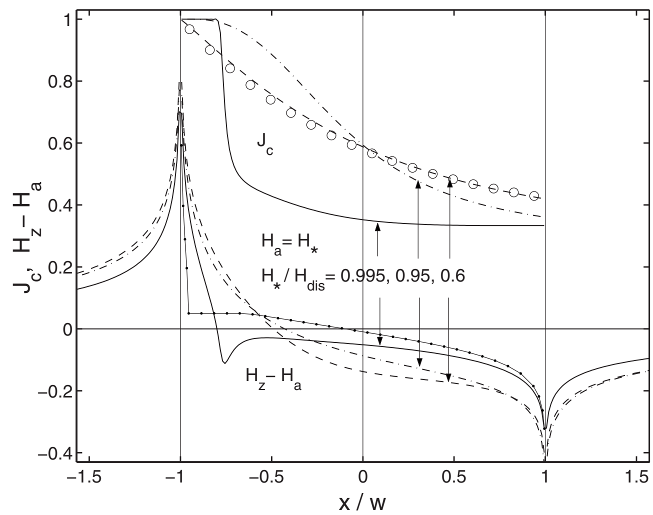

FIG. 3. Profiles of the critical sheet current $J_c(x)$ and magnetic field $H_z(x)$ in the strip within the contamination-annealing model at $H_a=H_*$ and for $H_*/H_{\rm dis}=0.6$ (dashed lines), 0.95 (dash-dot lines), and 0.995 (solid lines). The open circles show the dependence [Eq. (20)] at $H_a=H_*$, i.e., at $L_a(H_a)=w$. The solid line with dots shows for comparison $H_z(x)$ for the local-equilibrium model at $H_a=0.995H_{\rm dis}$. The sheet current and the magnetic field are measured in units of J_{c2}; $J_{c1}/J_{c2}=1/3$, $\gamma=2.6$, and $H_{\rm dis}=10J_{c2}$.

The critical states in the strip depend on the relationship between J_{c1} or J_{c2}, and the scale $H_{\rm dis}-H_*$. This relationship can be different for different superconductors and generally changes with the temperature.[47] If the sheet currents J_{c1} and J_{c2} are small as compared to $H_{\rm dis}-H_*$, $J_{c1}, J_{c2} \ll H_{\rm dis}-H_*$, one may neglect the self fields of the currents and put $L_a(H_z)\approx L_a(H_a)$ in Eq. (17). Then,

$$J_c(x) = \Delta J_c \exp\left[-\frac{x+w}{L_a(H_a)}\right] + J_{c1}, \tag{20}$$

and the dc critical current $I_c=\int_{-w}^{w}J_c(x)dx$ of the strip is given by the formula

$$I_c = \Delta J_c L_a(H_a)\left\{1-\exp\left[-\frac{2w}{L_a(H_a)}\right]\right\} + 2wJ_{c1}. \tag{21}$$

Expressions (20) and (21), were, in fact, derived in Ref. 36. The difference between formulas (20) and (21) and those of Ref. 36 is only that Paltiel *et al.* considered the dynamic annealing, their annealing length L_a increased with decreasing E_c and was not described by formula (18), i.e., it did not approach zero at $v=(E_c/B_a)\to 0$. The profiles $J_c(x)$ and $H_z(x)$ calculated within the contamination-annealing model in the case $H_{\rm dis}-H_*=4J_{c2}$ are shown by the dashed lines in Fig. 3. It is seen that these profiles indeed can be obtained from formula (20) as shown by the open circles.

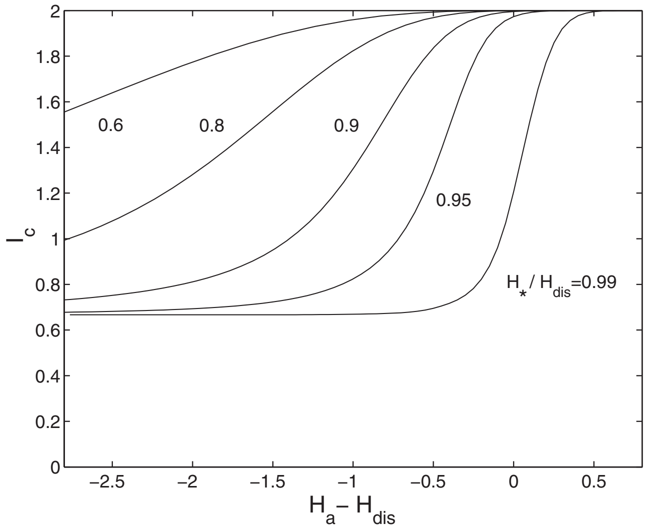

FIG. 4. The magnetic field dependence of the critical current I_c of the strip within the contamination-annealing model at $J_{c1}/J_{c2}=1/3$ and for H_*/H_{dis}=0.6, 0.8, 0.9, 0.95, and 0.99. The critical current I_c is measured in units of wJ_{c2} and the external magnetic field H_a in units of J_{c2}. Here $H_{\mathrm{dis}}=10J_{c2}$ and $\gamma=2.6$.

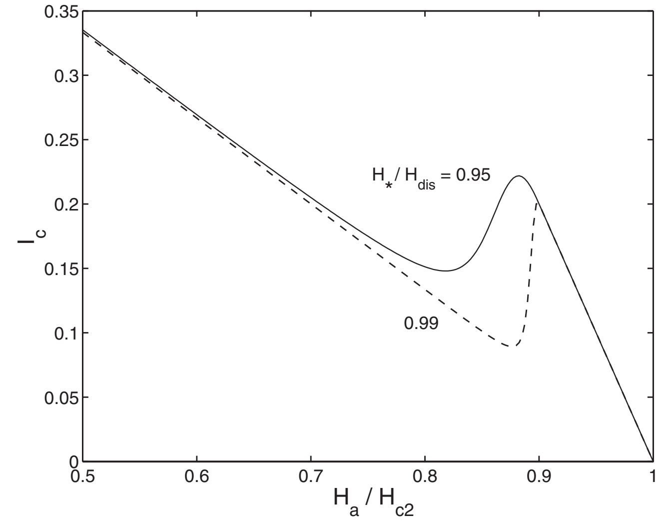

FIG. 5. The magnetic field dependence of the critical current I_c of the strip within the contamination-annealing model at H-dependent sheet currents $J_{c1}(H)=J_{c1}(0)[1-(H/H_{c2})]$ and $J_{c2}(H)=J_{c2}(0)[1-(H/H_{c2})]$ in the case J_{c1} and $J_{c2}\ll H_{\mathrm{dis}}-H_*$. Equations (1), (18), (19), and (21) have been used with $H_{\mathrm{dis}}=0.9H_{c2}$, $J_{c1}(0)/J_{c2}(0)=1/3$, $\gamma=2.6$, and H_*/H_{dis}=0.95 and 0.99. The critical current I_c is measured in units of $wJ_{c2}(0)$ and the external magnetic field H_a in units of the upper critical field H_{c2}. Note that the shape of $I_c(H_a)$ depends on the width of the strip $2w$ and the threshold E_c via the parameter H_*/H_{dis}.

In the opposite limiting case $J_{c1}, J_{c2}\gg H_{\mathrm{dis}}-H_*$, any small deviation of the local magnetic field from H_* with variation of x leads to a sharp change of τ_a, and so at $H(x)>H_*$ one has $\tau_a, L_a\to\infty$, and hence $J_c(x)\to J_{c2}$, while at $H(x)<H_*$ the annealing time τ_a and the annealing length L_a sharply decrease and $J_c(x)\to J_{c1}$. In fact, we arrive at a situation similar to the local equilibrium model (2), but now the jump of J_c occurs in a narrow interval near H_* instead of the point H_{dis}. Of course, the shape of the spatial profiles $J_c(x)$ and $H_z(x)$ with full details depends on the law, Eqs. (1) and (18), describing this jump of the sheet current. But when the parameter $(H_{\mathrm{dis}}-H_*)/J_{c1}$ decreases, these profiles tend to the results obtained within the local-equilibrium approach, Fig. 3. In other words, in the sample there is an extended spatial region in which $H_z(x)$ is almost a constant close to H_{dis} (the variation of H_z in this region is of the order of $H_{\mathrm{dis}}-H_*$), and $J_c(x)$ changes gradually from J_{c2} to J_{c1}. This result is also understood from the fact that the case $H_*/H_{\mathrm{dis}}\to 1$ can be always interpreted as the limit $\tau_0\to 0$. But in this limit the dependence $\tau_a(B_z)$ for the contamination-annealing model tends to the dependence appropriate to local equilibrium approach, see Sec. I.

In the general case the profiles $J_c(x)$ and $H_z(x)$ can be calculated with equations Eqs. (1), (3), and (17)–(19), and in Fig. 3, we show the evolution of these profiles with changing H_*/H_{dis}. The H_a dependences of the critical current I_c for different relationships between the sheet currents J_{c1}, J_{c2}, and $H_{\mathrm{dis}}-H_*$ are presented in Fig. 4.

Interestingly, if a current I is applied to the strip in the initially ordered state rather than a constant electric field, and if this current lies in the interval between $2wJ_{c1}$ and I_c, $2wJ_{c1}\le I\le I_c$, a nonzero electric field E appears at the initial stage of the process after the current is switched on, but this E decays and tends to zero as a steady distribution of the disordered phase is established in the sample. This transient process was experimentally investigated in Ref. 33, and was theoretically analyzed by Marchevsky *et al.*[48] in the case when $L_a\gg 2w$.

The above results were derived assuming that thermal annealing of the metastable disordered states is realized in the sample. This implies that at $E=E_c$ the dynamic annealing length L_a^{dyn} is essentially larger than the thermal annealing length L_a^{th} described by Eq. (18). If the opposite relationship $L_a^{\mathrm{dyn}}\ll L_a^{\mathrm{th}}$ holds at $E=E_c$, the disordered phase is mainly annealed by the vortex motion, while at $L_a^{\mathrm{dyn}}\sim L_a^{\mathrm{th}}$ both annealing mechanisms take place. In these situations the above formulas except Eq. (18) remain true. For the dynamic annealing the length $L_a(B_z)$ is given by a decreasing function of E_c (Refs. 30 and 36) rather than by the simple formula (18). This property of $L_a(E_c)$ can be used to distinguish between the mechanisms of the annealing in the sample. In particular, the field H_* near which the increase of the critical current $I_c(H_a)$ occurs increases with increasing E_c for the dynamic annealing and decreases for the thermal annealing. Thus, with changing E_c the peak in $I_c(H_a)$ deforms in opposite directions for these two cases.

Example: The peak effect

The equations and formulas presented in this paper enable one to calculate the shape of the dc critical current I_c versus the applied magnetic field H_a in the vicinity of the peak effect or the second magnetization peak if some H dependences of J_{c1} and J_{c2} are incorporated into the contamination-annealing model. As an example, in Fig. 5 we show $I_c(H_a)$ in the simple case when J_{c1} and J_{c2} are proportional to $1-(H/H_{c2})$ in the region of the peak effect and when the self-magnetic-field of the critical current is negligible. In the construction of this figure we have implied that the thermal annealing plays the main role in the sample, and $\tau_a(B_z)$ is described by Eq. (1). Note that with increasing E_c (i.e., with decreasing $H_*/H_{\rm dis}$ for the case of the thermal annealing) the peak in I_c shifts to lower magnetic fields in accordance with the prediction given above.

V. CONCLUSIONS

In this paper, we have investigated the critical states and the dc critical current of a superconducting strip near the order-disorder transition within the contamination-annealing model and with consideration for the self-magnetic-field of the current. In this model the metastable disordered states are taken into account, and their relaxation is determined by the parameter $H_*/H_{\rm dis}$. When this parameter approaches unity, i.e., when the relaxation occurs in a narrow magnetic-field interval, the obtained results tend to those of the local-equilibrium model for which explicit analytical formulas have been derived. The equations and formulas of this paper permit one to describe quantitatively the peak and fishtail effects observed in type-II superconductors.

ACKNOWLEDGMENTS

This work was supported by the German Israeli Research Grant Agreement (GIF) under Grant No. G-901-232.7/2005. E.Z. acknowledges the support of EU-FP7-ERC-AdG and of U.S.–Israel Binational Science Foundation (BSF).

[1] R. Wördenweber, P. H. Kes, and C. C. Tsuei, Phys. Rev. B **33**, 3172 (1986); R. Wördenweber and P. H. Kes, Cryogenics **29**, 321 (1989).

[2] S. Bhattacharya and M. J. Higgins, Phys. Rev. Lett. **70**, 2617 (1993).

[3] M. J. Higgins and S. Bhattacharya, Physica C **257**, 232 (1996).

[4] Y. Paltiel, E. Zeldov, Y. N. Myasoedov, H. Shtrikman, S. Bhattacharya, M. J. Higgins, Z. L. Xiao, E. Y. Andrei, P. L. Gammel, and D. J. Bishop, Nature (London) **403**, 398 (2000).

[5] Y. Paltiel, E. Zeldov, Y. Myasoedov, M. L. Rappaport, G. Jung, S. Bhattacharya, M. J. Higgins, Z. L. Xiao, E. Y. Andrei, P. L. Gammel, and D. J. Bishop, Phys. Rev. Lett. **85**, 3712 (2000).

[6] M. Marchevsky, M. J. Higgins, and S. Bhattacharya, Nature (London) **409**, 591 (2001).

[7] S. S. Banerjee, A. K. Grover, M. J. Higgins, G. I. Menon, P. K. Mishra, D. Pal, S. Ramakrishnan, T. V. Chandrasekhar Rao, G. Ravikumar, V. C. Sahno, S. Sarkar, and C. V. Tomy, Physica C **355**, 39 (2001).

[8] G. Yang, P. Shang, S. D. Sutton, I. P. Jones, J. S. Abell, and C. E. Gough, Phys. Rev. B **48**, 4054 (1993).

[9] Y. Yeshurun, N. Bontemps, L. Burlachkov, and A. Kapitulnik, Phys. Rev. B **49**, 1548 (1994).

[10] L. Klein, E. R. Yacoby, Y. Yeshurun, A. Erb, G. Müller-Vogt, V. Breit, and H. Wühl, Phys. Rev. B **49**, 4403 (1994).

[11] A. A. Zhukov, H. Küpfer, H. Claus, H. Wühl, M. Kläser, and G. Müller-Vogt, Phys. Rev. B **52**, R9871 (1995).

[12] M. Jirsa, L. Pust, D. Dlouhý, and M. R. Koblischka, Phys. Rev. B **55**, 3276 (1997).

[13] G. K. Perkins, L. F. Cohen, A. A. Zhukov, and A. D. Caplin, Phys. Rev. B **55**, 8110 (1997).

[14] K. Deligiannis, P. A. J. de Groot, M. Oussena, S. Pinfold, R. Langan, R. Gagnon, and L. Taillefer, Phys. Rev. Lett. **79**, 2121 (1997).

[15] H. Küpfer, Th. Wolf, C. Lessing, A. A. Zhukov, X. Lançon, R. Meier-Hirmer, W. Schauer, and H. Wühl, Phys. Rev. B **58**, 2886 (1998).

[16] T. Nishizaki, T. Naito, and N. Kobayashi, Phys. Rev. B **58**, 11169 (1998).

[17] S. Kokkaliaris, P. A. J. de Groot, S. N. Gordeev, A. A. Zhukov, R. Gagnon, and L. Taillefer, Phys. Rev. Lett. **82**, 5116 (1999); S. Kokkaliaris, A. A. Zhukov, P. A. J. de Groot, R. Gagnon, L. Taillefer, and T. Wolf, Phys. Rev. B **61**, 3655 (2000).

[18] D. Giller, A. Shaulov, Y. Yeshurun, and J. Giapintzakis, Phys. Rev. B **60**, 106 (1999).

[19] T. Nishizaki, T. Naito, S. Okayasu, A. Iwase, and N. Kobayashi, Phys. Rev. B **61**, 3649 (2000).

[20] H. Küpfer, Th. Wolf, R. Meier-Hirmer, and A. A. Zhukov, Physica C **332**, 80 (2000).

[21] M. Pissas, S. Lee, A. Yamamoto, and S. Tajima, Phys. Rev. Lett. **89**, 097002 (2002).

[22] M. Zehetmayer, M. Eisterer, J. Jun, S. M. Kazakov, J. Karpinski, B. Birajdar, O. Eibl, and H. W. Weber, Phys. Rev. B **69**, 054510 (2004).

[23] B. Khaykovich, E. Zeldov, D. Majer, T. W. Li, P. H. Kes, and M. Konczykowski, Phys. Rev. Lett. **76**, 2555 (1996).

[24] N. Avraham, B. Khaykovich, Y. Myasoedov, M. Rappaport, H. Shtrikman, D. E. Feldman, T. Tamegai, P. H. Kes, M. Li, M. Konczykowski, K. van der Beek, and E. Zeldov, Nature (London) **411**, 451 (2001).

[25] H. Beidenkopf, N. Avraham, Y. Myasoedov, H. Shtrikman, E. Zeldov, B. Rosenstein, E. H. Brandt, and T. Tamegai, Phys. Rev. Lett. **95**, 257004 (2005).

[26] G. P. Mikitik and E. H. Brandt, Phys. Rev. B **64**, 184514 (2001).

[27] T. Giamarchi and P. Le Doussal, Phys. Rev. B **55**, 6577 (1997).

[28] R. D. Merithew, M. W. Rabin, M. B. Weissman, M. J. Higgins, and S. Bhattacharya, Phys. Rev. Lett. **77**, 3197 (1996).

[29] S. N. Gordeev, P. A. J. de Groot, M. Oussena, A. V. Volkozub, S. Pinfold, R. Langan, R. Gagnon, and L. Taillefer, Nature (London) **385**, 324 (1997).

[30] W. Henderson, E. Y. Andrei, M. J. Higgins, and S. Bhattacharya, Phys. Rev. Lett. **77**, 2077 (1996).

[31] S. S. Banerjee, N. G. Patil, S. Ramakrishnan, A. K. Glover, S. Bhattacharya, G. Ravikumar, P. K. Mishra, T. V. Chandrasekhar Rao, V. C. Sahni, and M. J. Higgins, Appl. Phys. Lett. **74**, 126 (1999).

[32] W. Henderson, E. Y. Andrei, and M. J. Higgins, Phys. Rev. Lett. **81**, 2352 (1998).

[33] Z. L. Xiao, E. Y. Andrei, and M. J. Higgins, Phys. Rev. Lett. **83**,

1664 (1999).

[34] Y. Paltiel, G. Jung, Y. Myasoedov, M. L. Rappaport, E. Zeldov, M. J. Higgins, and S. Bhattacharya, Europhys. Lett. **58**, 112 (2002).

[35] S. Mohan, J. Sinha, S. S. Banerjee, A. K. Sood, S. Ramakrishnan, and A. K. Grover, Phys. Rev. Lett. **103**, 167001 (2009).

[36] Y. Paltiel, Y. N. Myasoedov, E. Zeldov, G. Jung, M. L. Rappaport, D. E. Feldman, M. J. Higgins, and S. Bhattacharya, Phys. Rev. B **66**, 060503(R) (2002).

[37] D. Giller, A. Shaulov, T. Tamegai, and Y. Yeshurun, Phys. Rev. Lett. **84**, 3698 (2000).

[38] C. J. van der Beek, S. Colson, M. V. Indenbom, and M. Konczykowski, Phys. Rev. Lett. **84**, 4196 (2000).

[39] B. Kalisky, D. Giller, A. Shaulov, and Y. Yeshurun, Phys. Rev. B **67**, 140508(R) (2003).

[40] B. Kalisky, A. Shaulov, and Y. Yeshurun, Phys. Rev. B **68**, 012502 (2003).

[41] B. Kalisky, Y. Bruckental, A. Shaulov, and Y. Yeshurun, Phys. Rev. B **68**, 224515 (2003).

[42] B. Kalisky, Y. Myasoedov, A. Shaulov, T. Tamegai, E. Zeldov, and Y. Yeshurun, Phys. Rev. Lett. **98**, 107001 (2007).

[43] M. V. Indenbom, E. H. Brandt, C. J. van der Beek, and M. Konczykowski, Phys. Rev. B **70**, 144525 (2004).

[44] I. M. Babich, G. P. Mikitik, and E. H. Brandt, Phys. Rev. B **74**, 224501 (2006).

[45] Conditions (2) and (4)–(6) mean that $J(x)$ and $H_z(x)$ are monotonically decreasing functions at least in the vicinities of the points $x=a_1$ and $x=a_2$. This requirement leads to the relationship [Eq. (9)] between a_1 and a_2. If a_1 were closer to a_2 than it follows from Eq. (9), $H_z(x)$ would increase near $x=a_2$ (Ref. 44).

[46] N. Muskhelishvili, *Singular Integral Equations* (Nordhoff, Groningen, Holland, 1953).

[47] For example, at temperature 27K and at $E_c \sim 10^{-4}$ V/m one has $J_{c2} \sim 700$ Oe in a BSCCO sample of the thickness 50 μm; see B. Kalisky, D. Giller, A. Shaulov, T. Tamegai, and Y. Yeshurun, Phys. Rev. B **72**, 014531 (2005). With increasing temperature, the currents J_{c2} and J_{c1} decrease.

[48] M. Marchevsky, M. J. Higgins, and S. Bhattacharya, Phys. Rev. Lett. **88**, 087002 (2002).